A PVA based thermochromic material for ultrasound therapy phantoms

Simone Ambrogio[1,2], Raphaela de Melo Baêsso[2], Alberto Gomis[2,3], Ian Rivens[3], [3]Gail ter Haar, Bajram Zeqiri[2], Kumar V Ramnarine[1], Fiammetta Fedele[1], Piero Miloro[2]

[1]Medical Physics Department, Guy's & St Thomas' NHS FoundationTrust, London, United Kingdom.

[2]Ultrasound and Underwater Acoustics, National Physical Laboratory, Hampton Road, Teddington, United Kingdom.

[3]Joint Department of Physics at The Institute of Cancer Research and The Royal Marsden NHS Foundation Trust, London, United Kingdom.

Corresponding Author: Simone Ambrogio (Simone.Ambrogio@gstt.nhs.uk; simoambr@gmail.com)

Abstract

Temperature estimation is a fundamental step to assess the efficacy of thermal therapy. A thermochromic material, sensitive within a temperature range of 52.5 °C - 75 °C has been developed. The material is based on PVA cryogel with the addition of a commercial thermochromic ink. It is simple to manufacture, low cost, non-toxic and versatile. The thermal response of the material was evaluated using multiple methods, including immersion in a temperature-controlled water bath, a temperature-controlled heated needle and High Intensity Focused Ultrasound (HIFU) sonication. Changes in colour were evaluated using both RGB maps and pixel intensities. Acoustic and thermal properties of the material were measured. Thermo-Acoustic simulations were run with an open-source software and results were compared with the HIFU experiments, showing good agreement. The material shows good potential for the development of ultrasound therapy phantoms.

Keywords: phantom, thermal ablation, thermochromic material, High Intensity Focused Ultrasound, quality assurance

Introduction

Thermochromic materials change colour with temperature. The change can be either reversible or permanent. They have been used to manufacture phantoms supporting studies of thermal therapies involving ultrasound, electromagnetic, radiofrequency, microwave, or optical radiation (Dabbagh et al. 2014a). Reversible changes have been obtained, for example, using thermochromic pigments (Butterworth 2012) or non-ionic surface-active agents, such as N-isopropylacrylamide (NIPAM) and PolyNIPAM (Dabbagh et al. 2014b).

Permanent changes in colour allow examination of the samples after an exposure, at the expense of showing only the maximum temperature reached in the experiments. Silicone-based materials have been developed (Costa et al. 2016), but polyacrylamide-based gels, formed of acrylamide monomer cross-linked using a polymerization agent, are the most common base for thermochromic materials (Choi et al. 2013). One of the concerns about these materials is that, whilst polyacrylamide is safe, its monomer is a neurotoxic substance, likely to be carcinogenic (Besaratinia and Pfeifer 2007).

Natural proteins such as Bovine Serum Albumin or Egg Albumin are commonly used as thermo-sensitive agents, to produce gels which are optically transparent. In recent years, thermochromic inks such as MB Magenta NH 60 °C concentrate (LCR Hallcrest, LLC, USA) have found application for both electromagnetic (Mikhail et al. 2016; Negussie et al. 2016) and ultrasound thermal phantoms (Eranki et al. 2019). The materials lose their transparency, but the colour change is gradual over a temperature range (usually around 10-20 °C).

Polyvinyl Alcohol (PVA) is a water-soluble synthetic polymer that can be manufactured into a crosslinked hydrogel with repeated freeze-thaw cycles. Because of its tuneable acoustic and physical properties, several ultrasound tissue-mimicking materials have been developed using different PVA-based recipes (Chu and Rutt 1997; Surry et al. 2004; Dineley et al. 2006; Cournane et al. 2010; Cannon et al. 2011; Ramnarine et al. 2014; Kokkalis et al. 2015; Zhou et al. 2017; Brüningk et al. 2019). The physical properties of the final cryogel depend on evaporation during mixing, freezing temperature, freezing holding time, thawing rate and number of freezing/thawing stages (Peppas and Stauffer 1991; Stauffer and Peppas 1992).

In this work we present a new permanent colour change thermochromic material based on PVA (TC-PVA). The benefits of using PVA include low cost, non-toxicity and the easiness of manufacturing it when compared to other gels as acrylamide (Eranki et al. 2019; Mikhail et al. 2016) and also the capability to produce large volumes.. Furthermore, before crosslinking, PVA is liquid at room temperature and can easily be mixed with thermochromic inks, as opposed to agar-based or gelatin-based materials. The acoustic and thermal properties were measured, and the colour change and melting point analysed. The size of lesions obtained by various exposures to a characterized focused ultrasound field was compared with acousto-thermal simulations.

Materials and methods

Preparation of the TC-PVA

The material is prepared using components listed in Table 1. With the exception of the thermochromic ink, all the components were mixed in a beaker and stirred continuously using a hotplate stirrer at approximately 700 rpm. The beaker was covered with aluminium foil to minimise evaporation, and the mixture was slowly heated to a temperature of 95 °C ± 1 °C. A thermocouple was used to monitor the temperature while the compounds were stirred at the target temperature for 30 minutes. The solution was then allowed to cool down unstirred at ambient room temperature. Once cooled, the thermochromic ink (Kromagen Magenta MB60-NH) was added and the mixture was

manually stirred gently to avoid bubble formation for a further 5 minutes. Finally, the solution was poured into dedicated moulds which were placed inside a commercial freezer with a timer to enable 5 freeze-thaw (Stauffer and Peppas 1992). Each cycle lasted 48h (24h ON – 24h OFF). Custom built moulds, of internal diameter 55 mm and two different heights of 20 mm and 30 mm, were used for the manufacturing of samples for acoustic and thermal measurements. Commercially available propylene tubes (Fisher Scientific, Leicestershire, UK) of internal diameter 25 mm and height of 115 mm were used to manufacture the samples for thermal response measurements.

Table 1: List of components and concentrations by weight percent (wt %) for the new TC-PVA.

Component	Concentration (wt %)	Supplier
Deionised water	76.50	----
Polyvinyl Alcohol (99+% hydrolysed, Mw 89000-98000)	10	Sigma-Aldrich
Glycerol (99+%, extra pure)	8	Acros Organics
Benzalkonium chloride (50 wt% aqueous solution)	0.5	Acros Organics
Kromagen Magenta MB60-NH	5	LCR Hallcrest LTD

Thermal response

To assess the relationship between temperature and colour change, an adaptation of the method described by Eranki et al. (2019) was used. The propylene tubes (Fisher Scientific, Leicestershire, UK) containing 20 mL of PVA based thermochromic material (TC-PVA) were submerged in a temperature-controlled water bath for fifteen minutes at temperatures ranging from 50 °C to 65 °C ± 1 °C. The tubes were removed from the water bath and allowed to cool down to room temperature (20 °C) before colour analysis.

An image of the different tubes was taken using a 12MP camera and a 240 by 164 pixel Region of Interest (ROI) for each tube was analysed in MATLAB (Mathworks, MA, USA). The average values and the standard deviation of red, green and blue intensities in the ROIs were calculated and compared.

The material melting point was assessed using the setup shown in Figure 1. The extremities of a needle were connected to the terminals of a 180 W digital power supply (RS Components LTD, Northants, UK). When electric current flows through the needle, electric energy is converted into heat through resistive losses in the material. A thermocouple was placed approximately in the centre of the needle and connected to a portable reader (OMEGA Engineering, CT, USA). The needle was pushed through a small (approximately 10x10x5 mm) TC-PVA sample, until the sample was in correspondence with the thermocouple junction (± 1 mm). The current was varied manually using the power supply controller to achieve the desired temperature. Once the target temperature was reached, the temperature was kept constant (± 1 %) for 5 s. The power supply was then switched off, and the sample removed and sectioned. Melting was defined as having occurred when a permanent hole in the sample specimen larger than the diameter of the needle was seen. The procedure was repeated at least twice for different TC-PVA samples for temperature ranging from 40 °C to 80 °C in steps of 5 °C.

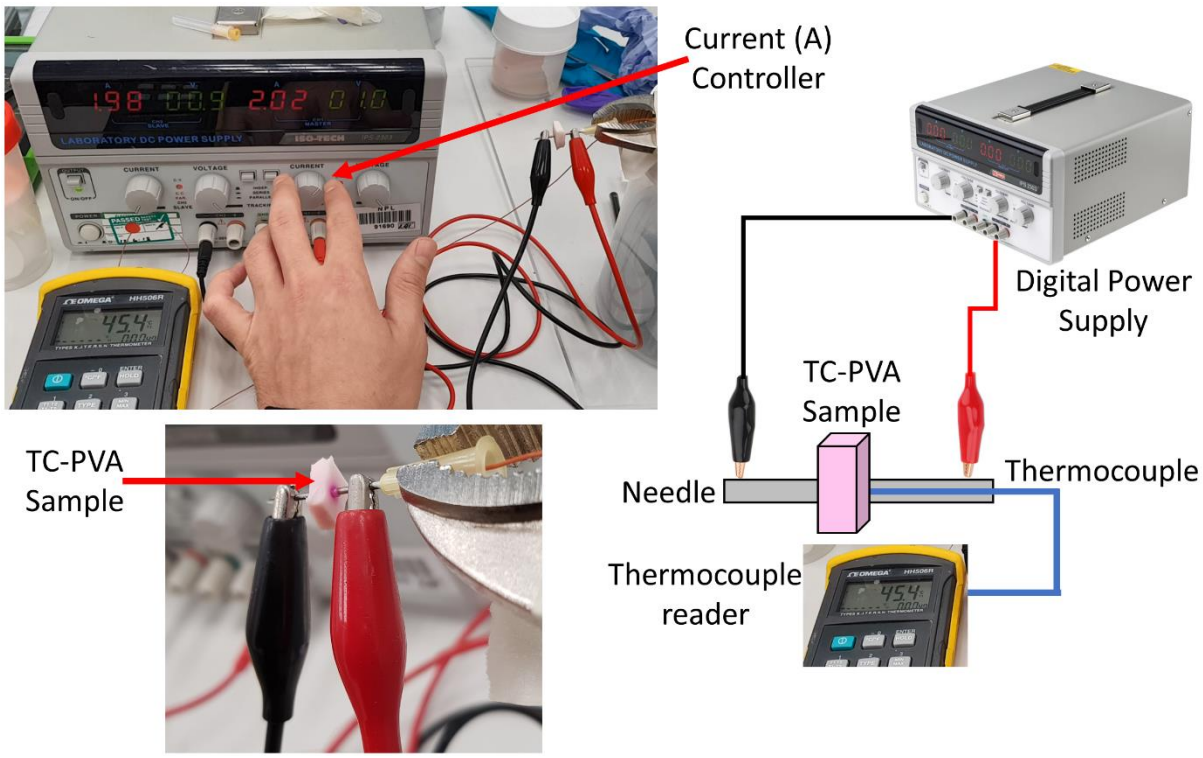

Figure 1- Temperature controlled needle experimental setup for the evaluation of colour change of the thermochromic PVA-based material.

Measurement of acoustic and thermal properties

Characterisation of the TC-PVA acoustic properties was performed at the National Physical Laboratory (NPL, Teddington, UK). Attenuation coefficient (*Att*) and speed of sound (*SoS*) were measured in the range 1 MHz to 20 MHz using a broadband through-transmission substitution technique. The method and the characterization facility are described by Rajagopal et al. (2015) and Zeqiri (2000). The method uses a single element broadband transducer (Force Technology, Brøndby, Denmark) with a 10 mm active element diameter as a transmitter, and a membrane hydrophone (GEC-Marconi, Essex, UK) with a sensitive element of 30 mm diameter as a receiver. Different samples with 55 mm diameter, and thicknesses of 20.5 mm and 32.5 mm, were placed into a custom-built acoustic holder with a 40 mm aperture.

Each sample was measured at four different separations in a range of 200 mm to 250 mm between the transducer and the sensor, and the results were averaged. The distance between the sample and the transducer was 60 mm. Water temperature was measured with a calibrated thermometer (IP 39C, G H Zeal LTD, London, UK) during the experiments, and was 20.0 °C ± 0.5 °C.

Thermal conductivity (*k*), diffusivity (*D*) and volumetric heat capacity (*cv*) were measured for each sample using a hand-held thermal property analyser (Tempos, METER Group, Pullman, USA). The SH-3 sensor of the analyser has two needles (dual-needle sensor) of length 30 mm and diameter 1.3 mm, separated by 6 mm. The needles were inserted into the material and data were collected for at least 30 s to determine the temperature drift. Once the drift was below a pre-set threshold, current was applied to one of the two needles (heater needle) for 30 s and temperature was monitored by the second needle (monitoring needle). After 30 s, current was switched off and temperature monitoring continued for a further 90 s. The starting temperature of the sample and the drift were then subtracted from the temperatures giving a temperature gradient that was used to calculate thermal conductivity (*k*), diffusivity (*D*) and volumetric heat capacity (*cv*) of the sample (Knight et al 2012). Before performing measurements on the TC-PVA samples, the SH-3 sensor was tested using a plastic Delrin cylinder as a

reference. Data were collected and results were compared with the values indicated by the Certificate of Quality Assurance of the Manufacturer.

Acoustic characterisation of the HIFU transducer

High Intensity Focused Ultrasound (HIFU) sonication were carried out using a 2 MHz single element HIFU transducer (H-106, Sonic Concepts, WA, USA) with a radius of curvature of 63.2 mm. The transducer was driven in continuous wave mode using a function generator (33220A, Agilent, CA, USA), in line with a power amplifier (150A100B, Amplifier Research UK, Buckinghamshire, UK). The transducer was characterised experimentally in degassed and deionised water using a calibrated needle hydrophone (0.2 mm, Precision Acoustics, UK). During characterization, the transducer was driven with a toneburst of 30 cycles. The drive voltage, monitored on an oscilloscope (MSOX3054T, Keysight Technologies, CA, USA), was 96 $V_{P\text{-}P}$. A 6 mm by 6 mm 2D scan was acquired in the focal plane, with step size 0.1 mm.

A further 27.6 mm by 27.6 mm 2D scan was carried out in the near field of the transducer, 12 mm pre-focally, with a step size of 0.3 mm. The pressure from the near field scan was used to evaluate the time averaged intensity, which was then integrated over the -24dB area to obtain the acoustic power, as described in IEC 62127-1 (IEC 2007).

HIFU exposures

A 20 mm thick, 55 mm dimeter sample was exposed to HIFU fields. The HIFU sonication setup used in the present study is shown in Figure 2.

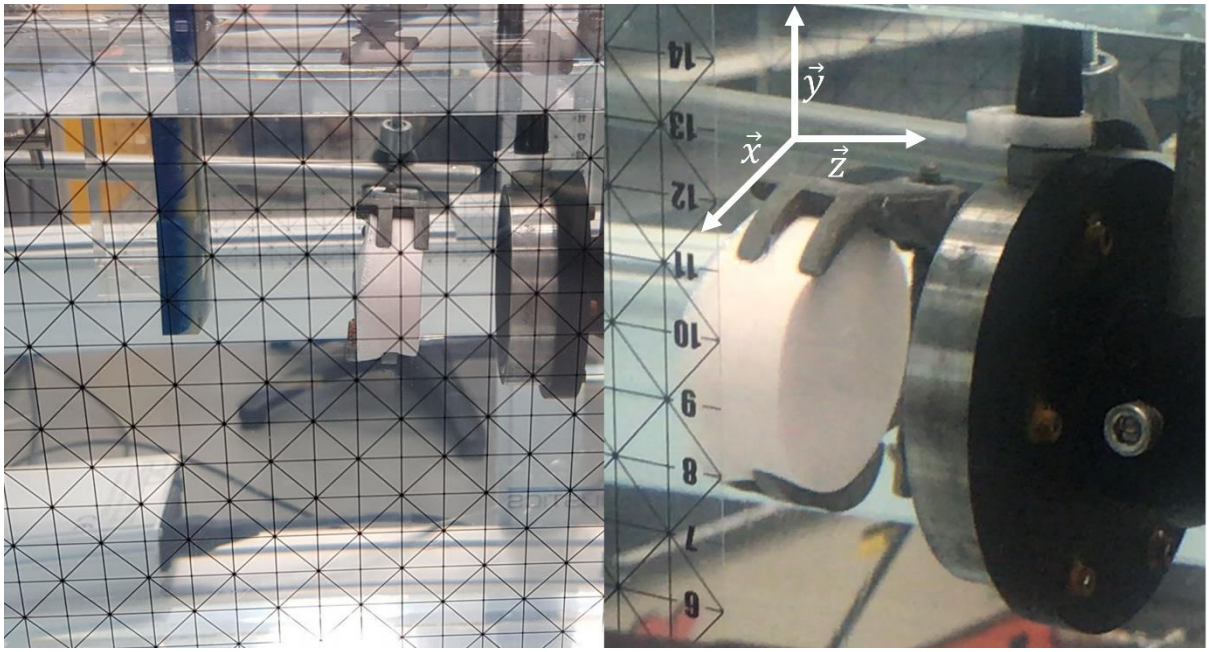

Figure 2 – HIFU exposures- experimental set-up. Sonication were performed by moving the HIFU H-106 transducer 5 mm along the *x*-axis, perpendicular to the beam-alignment axis of the transducer

A total of seven sonication locations were performed as shown in Figure 3. The needle hydrophone used for characterization was used to ensure that the focal plane of the transducer was within the sample, nominally at half its depth.

The sample was moved along an axis perpendicular to the beam axis in 5 mm increments, and each sonication was carried out with different exposure conditions as shown in Table 2. After each

sonication a 5 min cool-down time was applied. Table 2 shows the configurations used in each sonication.

Sonication 1 and 7 (Table 2) were carried out using higher acoustic powers in order to facilitate identification of the direction of the beam axis for later cutting. The large lesion resulting from high acoustic power sonications (1 and 7), resulted in visible spots on the back surface, which were used to facilitate cutting of the TC-PVA block perpendicular to the transducer beam axis. Sonication 2 to 6 were performed with the H-106 transducer being driven with the same voltage (96 $V_{p\text{-}p}$) but different exposure times, at different target locations.

After completing all sonication, the sample was cut using a sharp knife, and images were taken. The cross-sectional image of the sample was postprocessed in MATLAB to estimate width and length of the regions of interests, using the pixel intensity of the as an indicator of the colour shade. A pixel intensity baseline was calculated by averaging ~300k points outside the acoustic exposures region.

Table 2 – Driving voltage ($V_{p\text{-}p}$) and exposure time (s) used for each sonication.

Target location	Drive Voltage ($V_{p\text{-}p}$)	Time of exposure (s)
1	192	10
2	96	20
3	96	30
4	96	40
5	96	50
6	96	60
7	192	10

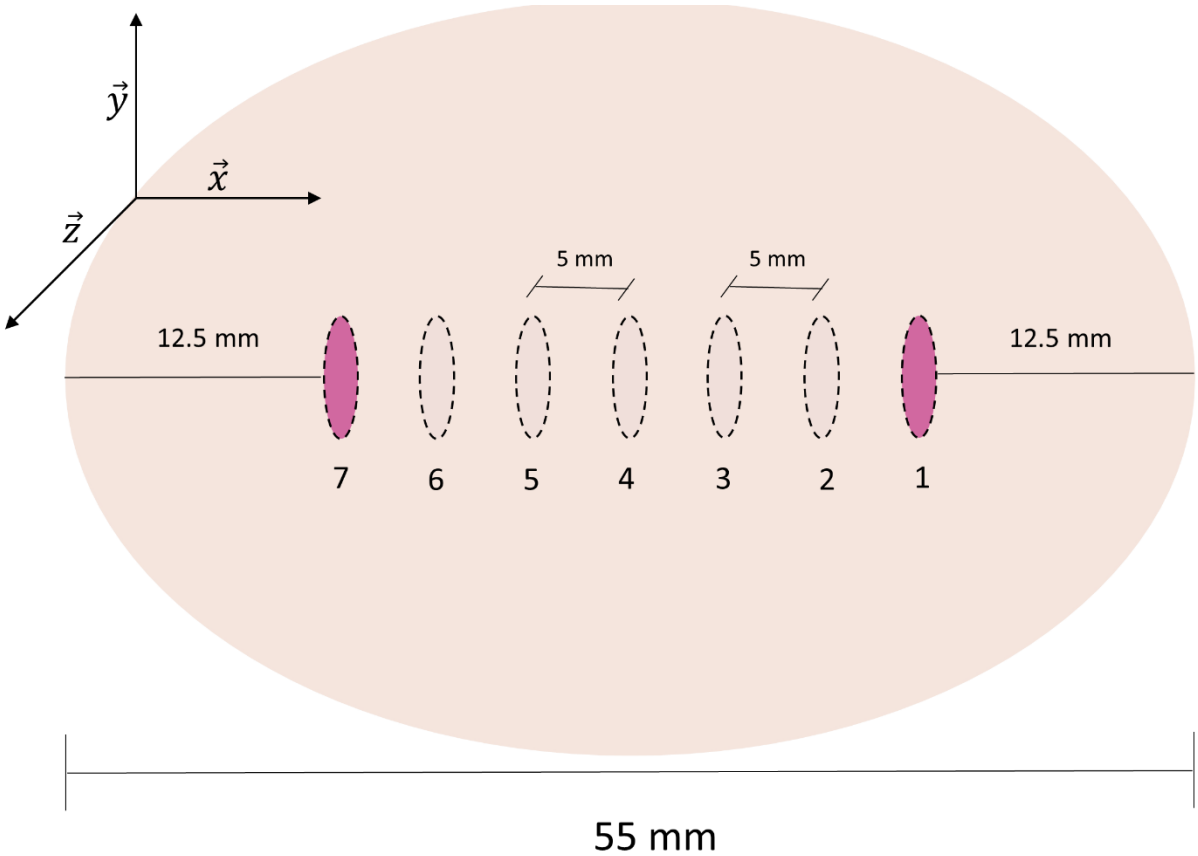

Figure 3 – Schematic diagram illustrating HIFU sonication in the TC-PVA sample. Drive voltage ($V_{p\text{-}p}$) and exposure time (s) for each target location are listed in Table 2.

Acousto-Thermal simulation of the acoustic field

Acousto-Thermal simulations were performed using HITU-Simulator v2.0 (Soneson 2020), a software package developed by the Food and Drug Administration (FDA) and freely available online. The software contains two main modules which can be modified/adapted from the user in MATLAB environment. The first module computes the wide-angle Khokhlov-Zabolotkaya-Kuznetsov equation (WAKZK), for calculating pressure distribution of an axisymmetric focused ultrasound transducer. The second module computes the bioheat transfer equation (BHT), for mapping heating and thermal dose distribution. The geometrical specifications of the transducer and the acoustic and thermal properties were used to specify the domain. As no scatters are added to the recipe, all of attenuation was attributed to absorption. Variations of the properties of the material with temperature were not considered. The acoustic power measured as described above was used as input for the field simulations. Thermal maps were obtained for exposure times of 20 s, 30 s, 40 s, 50 s and 60 s. A 60 s cooling time was computed after the end of each exposure.

Results

Thermal response

Figure 4 (b – e) shows the colour change of TC-PVA samples after 15 min exposure to water bath heating at four different temperatures (50 °C; 55 °C; 60 °C; 65 °C) in comparison to an unheated phantom sample (a). Intensity curves for colour and temperature show the RGB values extracted in Figure 4f.

The results in Figure 4 show a clear drop of the green component of the RGB intensity between 50 °C and 55 °C. The melting point, evaluated as described in the previous section, was found to be between 70 °C and 75 °C.

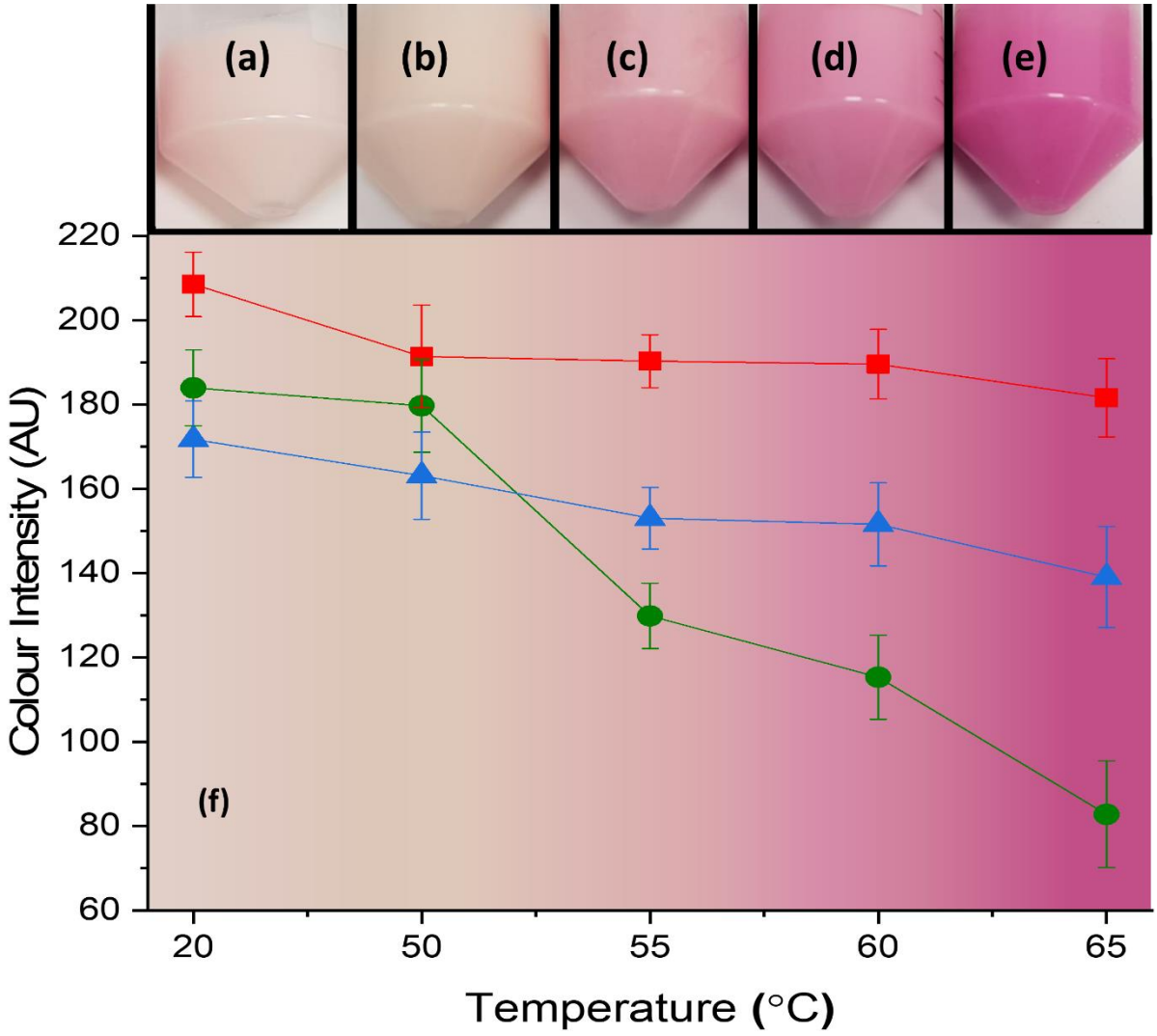

Figure 4 - Colour of TC-PVA samples (a) without heating and after 15 min water bath heating temperatures (b) 50 °C, (c) 55 °C, (d) 60 °C, (e) 65 °C and associated intensity curves for colour and temperature relation quantifying the RGB colour (■) red, (●) green and (▲) blue channel values. Colour intensity (AU) and error bars in the figure refer to average and standard deviation values calculated on 50,000 points selected from the sample image.

Measurement of acoustic and thermal properties

The acoustic properties of TC-PVA are shown in Figure 5. The values are reported with expanded measurement uncertainty (U), determined using both Type A (random) and Type B (systematic) uncertainty evaluations and a coverage factor of (p = 0.95), as described by Baêsso et al. (2019).

The attenuation was fitted as a function of frequency to a power law expression in the form of $y = a f^n$. The coefficients a and n for the TC-PVA samples are 0.13 and 1.5 respectively.

Table 3 summarizes the results in comparison with typical soft tissues for acoustic and thermal properties. The uncertainty quoted by the manufacturer for the three thermal parameters is 10%.

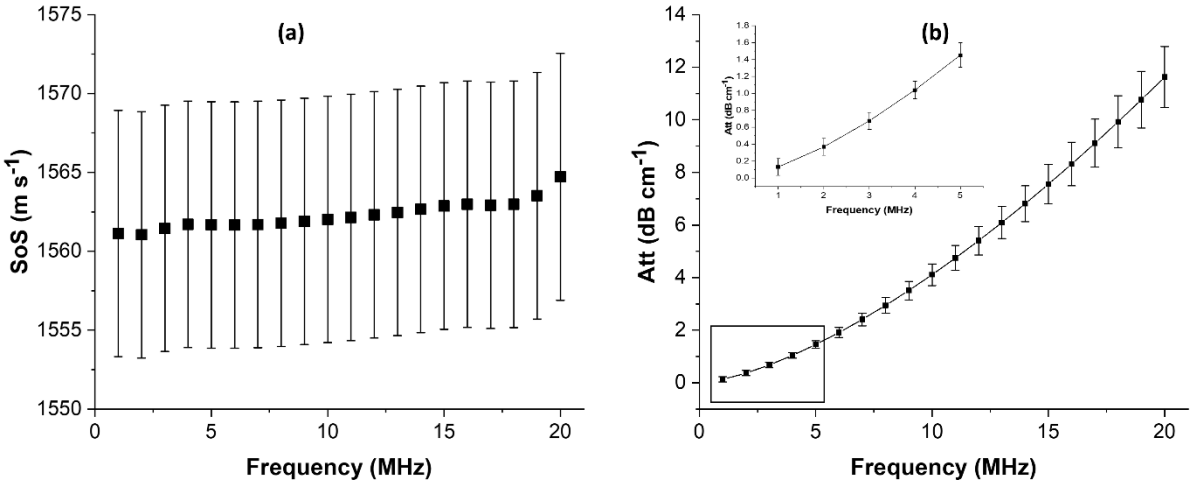

Figure 5 – Acoustic properties of TC-PVA measured in the 1 – 20 MHz range. Speed of Sound (*SoS*) and Attenuation (*Att*). Repeated measurements were performed on two samples of 55 mm diameter and thicknesses of 20.5 and 32.5mm.

Table 3 – Acoustic and Thermal properties for TC-PVA and soft tissues.

ACOUSTIC PROPERTIES

	Power fit: $Att = af^n$					SoS (m s^{-1})	
	a (dB cm^{-1} MHz^{-n})		n		Att (dB cm^{-1})		
Sample	Mean	Std	Mean	Std	2 MHz	Mean	Std
TC-PVA*	0.13	0.01	1.50	0.01	0.37	1562	12
Muscle (porcine) [(a)]**	0.54	0.14	1.33	0.06	1.36	1578	28
Skin with fat (porcine)[(a)]**	0.37	0.11	1.72	0.28	1.22	1486	15
Skin (porcine) [(b)]**	0.22	0.19	1.15	0.25	0.49	1631	35
Brain (human) [(c)]	---	---	---	---	---	1546	20
Kidney (human) [(c)]	---	---	---	---	---	1555	18

THERMAL PROPERTIES

Sample	k (W m^{-1} K^{-1})	D (mm^2 s^{-1})	c_v (MJ m^{-3}K^{-1})	T (° C)
TC-PVA	0.59	0.16	3.72	19.3
Muscle (porcine) [(a)]	0.46	0.16	---	37.0
Skin with fat (porcine) [(a)]	0.33	0.11	---	37.0
Brain (human) [(c)]	0.51	---	3.80	---
Kidney (human) [(c)]	0.53	---	4.01	---

Liver (human) [(d)]	0.52	0.14	---	---
Skin (human) [(e)]	0.37	0.04 – 0.16	---	---

*Measured at 20 °C and valid in the range of 1 – 20 MHz.

**Measured at 37 °C.

(a)(El-Brawany et al. 2009; (b)Hoskins 2007; (c) Hasgall et al. 2018 (d) Benjamin M. Davis, Glen F. Rall 2017; (e) Giering; et al. 1995)

Acoustic characterisation of the HIFU transducer

Fig. 6 shows the results of the acoustic characterization of the HIFU transducer.

The focal length was found to be 64.5 mm (from the concave surface of the transducer). Peak-positive acoustic pressure in the focal plane and in the near field (used to evaluate the power) are shown. The peak-positive and peak-negative acoustic pressures in the focal plane are also shown in comparison with simulation results. Figure 6 (c) and (d) show the peak-positive and peak-negative acoustic pressures in the focal plane derived using a calibrated hydrophone, and the results of the simulation in water.

The power evaluated from the raster scan in the near field was 12.05 W for a drive voltage of 96 V_{P-P}.

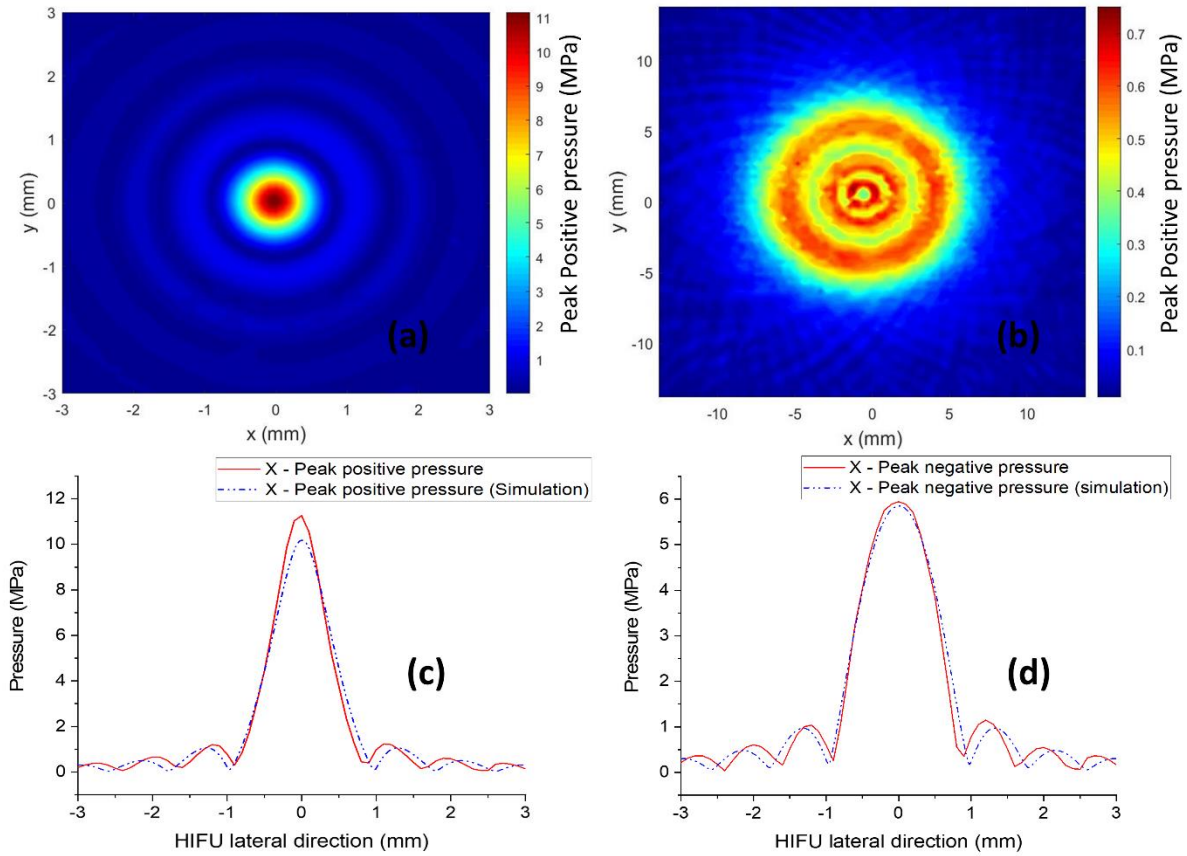

Figure 6 – Acoustic field characterisation of the 2.0 MHz HIFU transducer (H106, Sonic Concepts, WA, USA) employed. Experimentally measured two-dimensional HIFU peak-positive pressure in the (a) focal plane and in the (b) near field with contour beam profiles along the lateral directions and one dimensional (c) peak-positive and (d) peak-negative acoustic pressures in the focal plane measured in water by the needle hydrophone, compared with the output of the simulation.

HIFU exposures

As previously described, seven spatial locations were targeted in each TC-PVA sample (Figure 3). The sectioned gel shows the resulting colour change at each location (Figure 7).

Exposure times longer than 40 s (positions 4 - 6) displayed signs of melting in the centre of the coloured area. This is not visible for shorter exposure times (2 and 3).

The intensity analysis is shown in Figure 8, in which the 5 sonicated areas are clearly identifiable. The image represents pixel intensity on a scale 0-255.The length and the width of each area were measured with reference to the central point of the focus and are reported in Table 4. The pixel intensity baseline, estimated to be 130 (± 8%) on 300k points, was subtracted from the intensity map. Therefore, the zero point on the colour bar corresponds to regions where the thermochromic function of the ink was either not activated or was not identifiable.

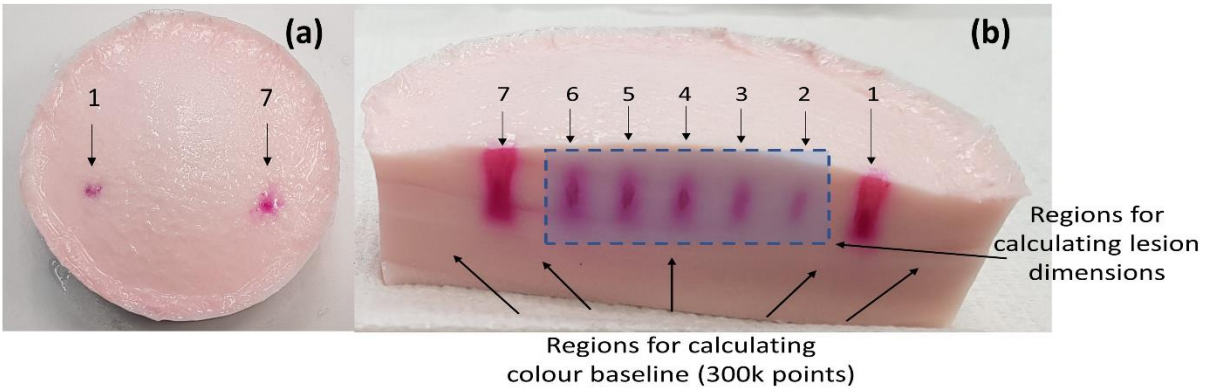

Figure 7 – Photograph of sonicated TC-PVA sample (a) rear surface before cutting and (b) after a perpendicular cut through the HIFU beam path showing the results of each sonication performed in this study.

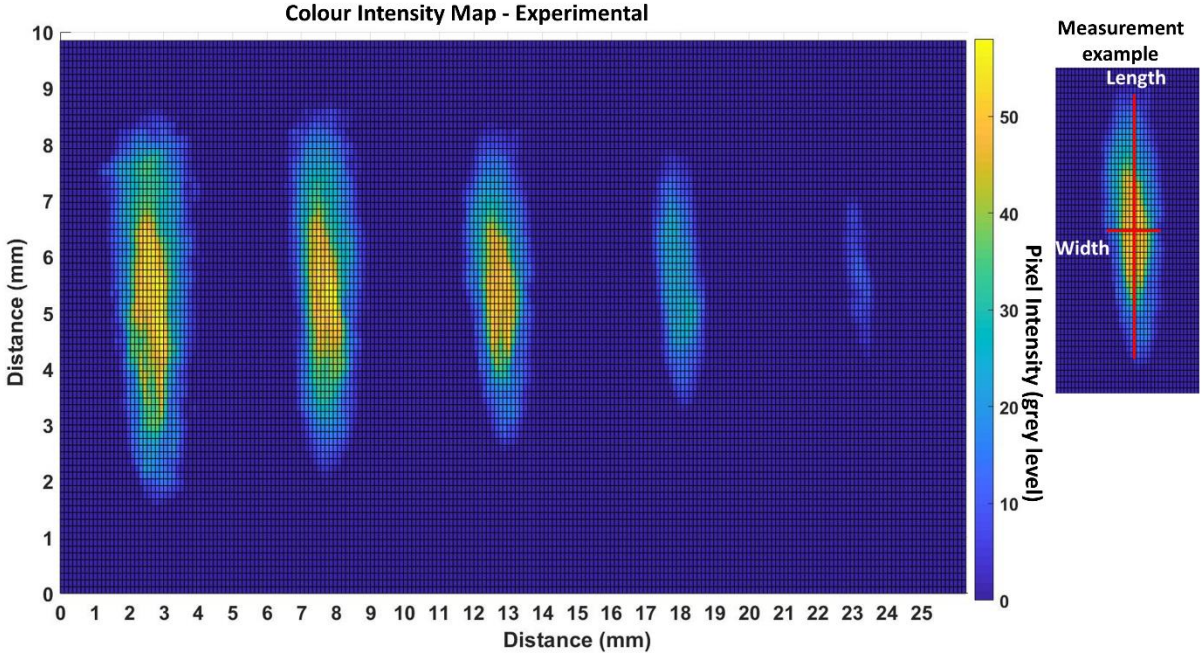

Figure 8. Intensity map of the 5 sonicated areas selected on Figure 7b. An example of how width and length measurements of the area were performed is also shown.

Acousto-thermal simulation of the acoustic field

The simulated temperature map after an exposure of 60 s is shown in Figure 9. The baseline temperature was set to 20 °C, corresponding to the initial sample temperature during experimental HIFU sonication. The peak temperature at the focus reached 78.3 °C. The time-temperature curves for the 5 exposures in the focus are also shown.

The region with temperatures above 52.5 °C was extracted for each simulated exposure time. The threshold of 52.5 °C was chosen as the mid-point between 50 °C and 55 °C, where the colour

intensity changes significantly (see also Figure 4). The widths and lengths of the regions were extracted and compared to the experimental results in Table 4.

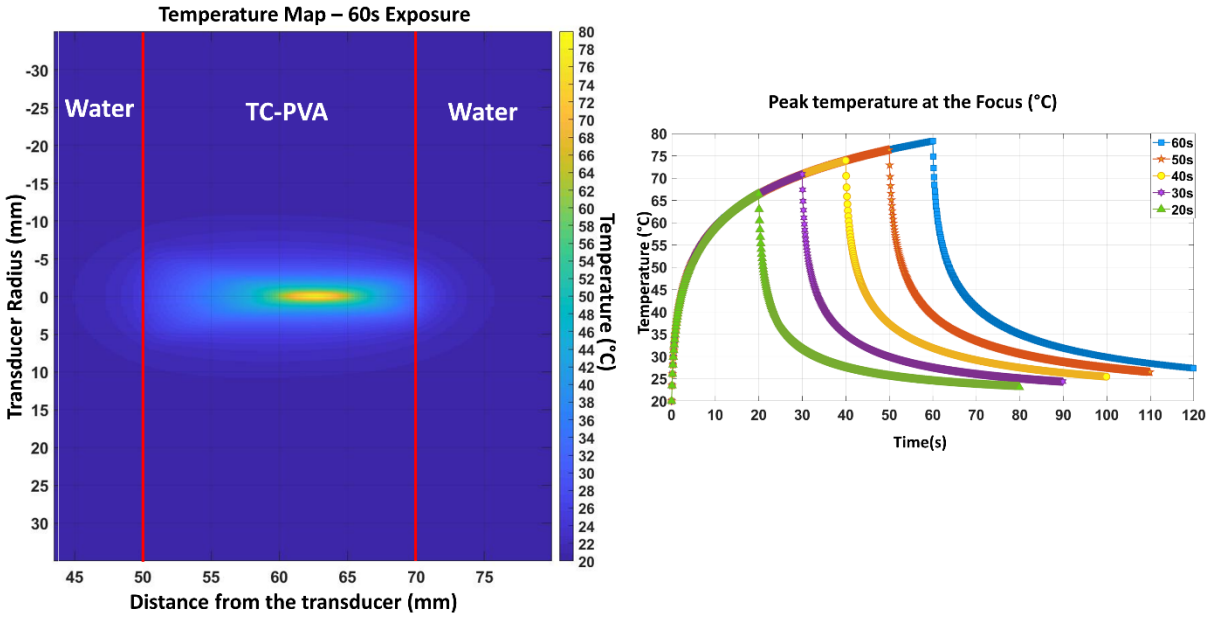

Figure 9. Temperature distribution after 60s exposure, and peak temperature at the focus simulated with HITU-Simulator v2.0 (Soneson 2020).

Table 4 – Comparison between experimental and simulated data for length and width.

Exposure Time (s)	Simulation			Experimental		Difference (simulation vs experimental)	
	Peak Temperature (°C)	Length (mm)	Width (mm)	Length (mm)	Width (mm)	Length (mm)	Width (mm)
20	66.5	4.2	1.2	3.1	0.8	1.1	0.4
30	70.1	5.1	1.6	4.6	1.4	0.5	0.2
40	74.0	5.7	1.8	5.6	1.9	0.1	-0.1
50	76.4	6.4	2.1	6.6	2.3	-0.2	-0.2
60	78.3	6.8	2.3	7.1	2.5	-0.3	-0.2

Discussion

In this paper we have presented a new thermochromic material based on PVA, with the addition of a thermochromic ink. The change in colour with temperature is non-reversible, which implies that the material is single use. The gel is easy to manufacture, cheap and non-toxic. The recipe did not include scatterers. This allowed the simplifying assumption that absorption is the main contribution to its attenuation, as the latter can be experimentally measured. Although this condition does not mimic realistic tissue properties, and the resulting attenuation is slightly lower than that of soft tissues, the choice is considered convenient for both simulation, thermal measurements and quality assurance.

The acoustic, thermal and mechanical properties of PVA materials can be tuned by varying the concentration of the components listed in Table 2, varying the number of freezing-thawing stages, or adding new ingredients. The addition of scatterers, such as Al_2O_3, SiC or TiO_2, can be explored to simulate soft tissue attenuation of approximately 0.5 dB cm^{-1} at 1 MHz (Rabell-Montiel et al. 2018).

Similar materials to the new TC-PVA have shown compatibility with ultrasound and Magnetic Resonance Imaging (Chu and Rutt 1997; Surry et al. 2004; Fortune et al. 2012), the two main modalities used for monitoring and guiding HIFU treatment in clinical practice.

The thermochromic material provides information about the geometry of the region in which the temperature exceeded a threshold. Rigorous quantification of temperature with change in colour requires more effort. However, two main target temperatures were identified: the activation temperature of the thermochromic ink, which is close to the target temperature for thermal ablation during clinical treatments with HIFU (56 °C for 1 s), and the melting point, which occurs between 70 and 75 °C.

The change in colour with temperature has been assessed using RGB intensities. The method is not quantitative, as it depends on different parameters such as the camera settings and ambient lighting levels in the room. However, a distinct change can be clearly observed between 50 °C and 55 °C.

The results of the simulation and the experimental data show good agreement, with an average difference of 0.2 mm on width and 0.6 mm on length in the size of the lesion. These values are higher for short exposures due to greater experimental uncertainty, for example errors due to the position of the cutting plane and pixel resolution. The melting point of the TC-PVA was found to be between 70 °C and 75 °C. Exposures of 40 s or longer at 12 W acoustic power show signs of producing gel melting and a simulated maximum temperature above 73 °C. There were no signs of melting for 20 s and 30 s exposures.

The material presented here may have several uses in medical ultrasound and more widely in thermal therapies (Fedele et al. 2019). These include validation of acousto-thermal simulations, testing of new ultrasound devices, quality assurance for existing systems, research and development of patient-specific 3-dimensional models for optimisation of HIFU treatments.

Acknowledgements

Authors acknowledge funding support from the National Measurements System, the UK Department for Business, Energy and Industrial Strategy, the Chief Scientific Office (England), the Therapy Ultrasound Network for Drug Delivery & Ablation Research (ThUNDDAR), The British Medical Ultrasound Society (BMUS) and Institute of Physics and Engineering in Medicine (IPEM).

References List

Baêsso RM, Costa-Felix RPB, Miloro P, Zeqiri B. Ultrasonic parameter measurement as a means of assessing the quality of biodiesel production. Fuel 2019;241.

Benjamin M Davis, Glen F, Rall MJS. Review of temperature dependence of thermal properties, dielectric properties, and perfusion of biological tissues at hyperthermic and ablation temperatures. Physiol Behav 2017;176:139–148.

Besaratinia A, Pfeifer GP. A review of mechanisms of acrylamide carcinogenicity. Carcinogenesis Oxford University Press, 2007;28:519–528.

Brüningk SC, Rivens I, Mouratidis P, ter Haar G. Focused Ultrasound-Mediated Hyperthermia in Vitro: An Experimental Arrangement for Treating Cells under Tissue-Mimicking Conditions. Ultrasound Med Biol 2019;45:3290–3297.

Butterworth I, Barrie J, Zeqiri B, Zauhar G, Parisot B. Exploiting thermochromic materials for the rapid quality assurance of physiotherapy ultrasound treatemnt heads. Ultrasound Med Biol 2012; 38:767-776.

Cannon LM, Fagan AJ, Browne JE. Novel tissue mimicking materials for high frequency breast ultrasound phantoms. Ultrasound Med Biol England, 2011;37:122–135.

Choi MJ, Guntur SR, Lee KIL, Paeng DG, Coleman A. A Tissue Mimicking Polyacrylamide Hydrogel Phantom for Visualizing Thermal Lesions Generated by High Intensity Focused Ultrasound.

Ultrasound Med Biol 2013;39:439–448.
Chu KC, Rutt BK. Polyvinyl alcohol cryogel: An ideal phantom material for MR studies of arterial flow and elasticity. Magn Reson Med John Wiley & Sons, Ltd, 1997;37:314–319.
Costa RM, Alvarenga A V, Costa-Felix RPB, Omena TP, von Krüger MA, Pereira WCA. Thermochromic Phantom and Measurement Protocol for Qualitative Analysis of Ultrasound Physiotherapy Systems. Ultrasound Med Biol Elsevier, 2016;42:299–307.
Cournane S, Cannon L, Browne JE, Fagan AJ. Assessment of the accuracy of an ultrasound elastography liver scanning system using a PVA-cryogel phantom with optimal acoustic and mechanical properties. Phys Med Biol England, 2010;55:5965–5983.
Dabbagh A, Abdullah BJJ, Abu Kasim NH, Ramasindarum C. Reusable heat-sensitive phantom for precise estimation of thermal profile in hyperthermia application. Int J Hyperth Taylor & Francis, 2014a;30:66–74.
Dabbagh A, Abdullah BJJ, Ramasindarum C, Abu Kasim NH. Tissue-mimicking gel phantoms for thermal therapy studies. Ultrason Imaging Sage Publications Sage CA: Los Angeles, CA, 2014b;36:291–316.
Dineley J, Meagher S, Poepping TL, McDicken WN, Hoskins PR. Design and characterisation of a wall motion phantom. Ultrasound Med Biol England, 2006;32:1349–1357.
El-Brawany MA, Nassiri DK, Terhaar G, Shaw A, Rivens I, Lozhken K. Measurement of thermal and ultrasonic properties of some biological tissues. J Med Eng Technol Taylor & Francis, 2009;33:249–256.
Eranki A, Mikhail AS, Negussie AH, Katti PS, Wood BJ, Partanen A. Tissue-mimicking thermochromic phantom for characterization of HIFU devices and applications. Int J Hyperth Taylor & Francis, 2019;36:518–529.
Fedele F, Zeqiri B, Butler D, Miloro P, Sinden D, Ilyas S, Monzon L, Abbas H, Bosio F, Thanou M, Gangi A. QUANTuM: A CSO Knowledge Transfer Partnership focusing on quality assurance in MR guided High Intensity Focused Ultrasound. Ultrasound, 2019; 27(2): NP1–NP52.
Fortune S, Jansen MA, Anderson T, Gray GA, Shneider JE, Hoskins PR, Marshal I, Anderson T. Development and characterization of rodent cardiac phantoms: comparison with in vivo cardiac imaging. Magnetic Resonance Imaging 2012; 30:1186-1191.
Giering K, Minet O, Lamprecht I, Muller G. Review of thermal properties of biological tissues. SPIE Opt Eng Press 1995;044:45–65.
Hasgall P, Di Gennaro F, Baumgartner C, Neufeld E, Lloyd B, Gosselin M, Payne D, Klingenböck A, Kuster N. IT'IS Database for thermal and electromagnetic parameters of biological tissues. 2018 [cited 2020 May 1].
Hoskins PR. Physical Properties of Tissues Relevant to Arterial Ultrasound Imaging and Blood Velocity Measurement. Ultrasound Med Biol 2007;33:1527–1539.
IEC. Ultrasonics - Hydrophones - Part 1: Measurement and characterization of medical ultrasonic fields up to 40 MHz, IEC 62127-1:2007. International Electrotechnical Commission, 2007. p. 166.
Knight J, Kluitenberg G, Kamai T, Hopmans J. Semianalytical solution for dual-probe heat-pulse applications that accounts for probe radius and heat capacity. Vadose Zone Journal 2012; 11.
Kokkalis E, Cookson AN, Stonebridge PA, Corner GA, Houston JG, Hoskins PR. Comparison of Vortical Structures Induced by Arteriovenous Grafts Using Vector Doppler Ultrasound. Ultrasound Med Biol Elsevier, 2015;41:760–774.
Mikhail AS, Negussie AH, Grahaman C, Mathew M, Wood BJ, Partanen A. Evaluation of a tissue-mimicking thermochromic phantom for radiofrequency ablation. Med Phys, 2016; 43:4304-4311.
Negussie AH, Partanen A, Mikhail AS, Xu S, Abi-Jaoudeh N, Maruvada S, Wood BJ. Thermochromic tissue-mimicking phantom for optimisation of thermal tumour ablation. Int J Hyperth Taylor & Francis, 2016;32:239–243.
Rabell-Montiel A, Anderson T, Pye SD, Moran CM. Attenuation Coefficients of the Individual Components of the International Electrotechnical Commission Agar Tissue-Mimicking Material.

Ultrasound Med Biol England, 2018;44:2371–2378.
Rajagopal S, Sadhoo N, Zeqiri B. Reference Characterisation of Sound Speed and Attenuation of the IEC Agar-Based Tissue-Mimicking Material Up to a Frequency of 60MHz. Ultrasound Med Biol 2015;41:317–333.
Ramnarine K V, Garrard JW, Dexter K, Nduwayo S, Panerai RB, Robinson TG. Shear wave elastography assessment of carotid plaque stiffness: in vitro reproducibility study. Ultrasound Med Biol England, 2014;40:200–209.
Soneson J. High intensity focused ultrasound simulator. MATLAB Central File Exchange, 2020.
Stauffer SR, Peppast NA. Poly(vinyl alcohol) hydrogels prepared by freezing-thawing cyclic processing. Polymer (Guildf) Elsevier, 1992;33:3932–3936.
Surry KJM, Austin HJB, Fenster A, Peters TM. Poly(vinyl alcohol) cryogel phantoms for use in ultrasound and MR imaging. Phys Med Biol England, 2004;49:5529–5546.
Zeqiri B BC. A new anechoic material for medical ultrasonic applications. Ultrasound Med Biol 2000;26:481–5.
Zhou X, Kenwright DA, Wang S, Hossack JA, Hoskins PR. Fabrication of Two Flow Phantoms for Doppler Ultrasound Imaging. IEEE Trans Ultrason Ferroelectr Freq Control United States, 2017;64:53–65.